Increased tortuosity of pulmonary arteries in patients with pulmonary hypertension in the arteries

Michael Pienn[1,2,*,†]
michael.pienn@lvr.lbg.ac.at
Christian Payer[1,2,*]
christian.payer@student.tugraz.at
Andrea Olschewski[1,3]
andrea.olschewski@lvr.lbg.ac.at
Horst Olschewski[1,4]
horst.olschewski@medunigraz.at
Martin Urschler[2,5]
martin.urschler@cfi.lbg.ac.at
Zoltán Bálint[1]
zoltan.balint@lvr.lbg.ac.at

[1] Ludwig Boltzmann Institute for Lung Vascular Research, Graz, Austria
[2] Inst. f. Computer Graphics & Vision Graz University of Technology, Austria
[3] Dep. of Experimental Anaesthesiology Medical University of Graz, Austria
[4] Department of Pulmonology Medical University of Graz, Austria
[5] Ludwig Boltzmann Institute for Clinical-Forensic Imaging, Graz, Austria

Abstract

Pulmonary hypertension (PH) is a chronic disorder of the pulmonary circulation, marked by an elevated vascular resistance and pressure. We hypothesised that, in patients with increased pressure in the arteries only, vessel tortuosity is more elevated in arteries than in veins. We present an automatic pulmonary vessel tree extraction algorithm, which identifies individual vessel trees. A vessel enhancement filter was used to find vertices along the vessel centrelines in the lung, which were connected to vessel trees using an integer program. For this proof-of-concept study, we used datasets of well-diagnosed patients, without comorbidities, where the identified vessel trees were manually labelled as either artery or vein. From these trees the tortuosity was calculated and compared to the patient's diagnosis and clinical data. In the arteries we found a higher difference in tortuosity than in the veins comparing patients with and without PH on the arterial side (1.036 ± 0.013 vs. 1.021 ± 0.001 in arteries and 1.026 ± 0.004 vs. 1.022 ± 0.001 in veins, respectively). We conclude that tortuosity is indeed a measure for the pressure in the respective vessels and might be a useful readout for non-invasive diagnosis of PH.

1 Introduction

Pulmonary hypertension (PH) is a disease characterised by elevated vascular resistance and blood pressure in the lung. PH results in a decreased exercise tolerance and typically leads to right-heart failure. It is diagnosed by right-heart catheterisation (RHC), which is the gold

[*] These authors contributed equally to the work.

[†] We thank Peter Kullnig for radiological, Gabor Kovacs, Vasile Fóris and Daniela Kleinschek for medical input.

standard method, where a mean pulmonary artery pressure (mPAP) $\geq$ 25 mmHg confirms its presence [3]. In several patients, the elevated pressure only resides in the pulmonary arteries, which is identified by a pulmonary artery wedge pressure $\leq$ 15 mmHg.

In order to replace the invasive RHC, a non-invasive alternative would be beneficial for the diagnosis of PH. Recently, Helmberger et al. have shown that morphologic analysis of the pulmonary vasculature, i.e. the analysis of how bent individual vessel segments are, can yield information on the presence of PH and might be a useful parameter for diagnosis [2]. As in certain subtypes of PH the hypertension is only present in the arteries, we investigated whether the tortuosity readout of the pulmonary arteries differs from that of the veins.

For this purpose, we developed a vessel tree extraction algorithm using a lung segmentation together with a vessel enhancement filter to obtain paths along the lung vasculature in contrast-enhanced thoracic computed tomography (CT) images. These paths are connected to individual vessel trees using an integer program. For this proof-of-concept study we manually annotated the resulting vessel trees as either arteries or veins, respectively. Finally, we calculated the vessel tortuosity for arteries and veins separately and compared them with the patient's diagnosis and clinical data derived from RHC.

1.1 Related Work

A large number of 3D vessel segmentation algorithms for investigating, e.g. pulmonary vessel trees, coronary arteries, or brain vessels have been presented in the literature. A recent, comprehensive overview of different techniques can be found in Lesage et al. [5]. Typical algorithms are based on vessel enhancement filters, which exploit that vessels have tube-like shape. These tubularity images are then used as an input for creating the vessel segmentation or for tracking the vessel trees. E.g Türetken et al. use a fast marching algorithm to connect vessel points identified from those tubularity images in order to create connected vessel graphs [6]. The analysis of complexity and tortuosity of the pulmonary vascular tree in patients with PH was presented in Helmberger et al. [2].

2 Method

Figure 1 shows the flowchart of our automatic vessel detection algorithm. We propose an algorithm that uses the whole thoracic CT dataset and starts with generating a lung segmentation, similar to [2]. All subsequent steps are performed for the left and the right lung independently. Vascular structures are enhanced with a multi-scale tubularity filter. We use the optimally-oriented flux (OOF) filter, proposed by Law and Chung [4] with an implementation from Benmansour et al. [1]. This multi-scale filter produces a vessel orientation estimate as well as a 4D tubularity image for the three spatial coordinates and the radius.

2.1 4D path graph

A local maxima graph $G = (V, E)$ is generated from the 4D vessel enhanced image. Each vertex $v_i \in V$ of the local maxima graph G corresponds to a local maximum in the enhanced image. We only use vertices with a high certainty of lying on the vessel centreline for vessels with diameters between 2 and 10 mm. These vertices are connected by edges within their local neighbourhood, where vertices $v_i \in V$ and $v_j \in V$ are connected by the edge $e_{ij} \in E$. The paths of these edges are constructed by minimising their geodesic distances, penalizing small

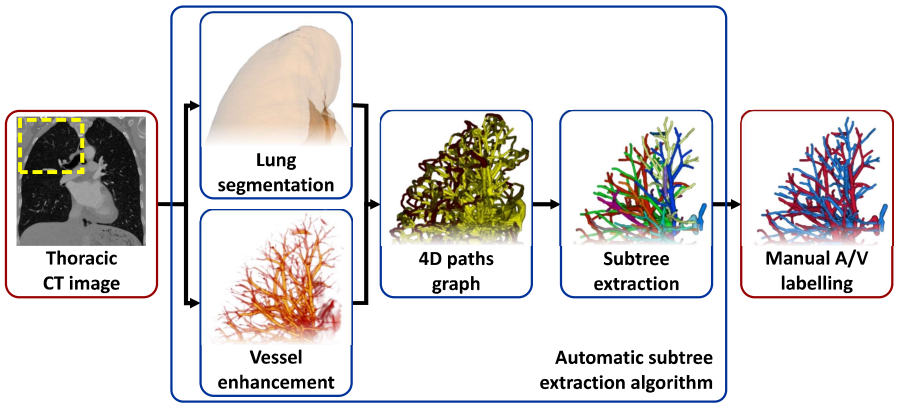

Figure 1: Vessel extraction flowchart. From the thoracic computed tomography (CT) image the lung is segmented and the vessels are marked using a vessel enhancement filter. These are used to generate an over-complete 4D path graph. Using an integer program the vessel subtrees are calculated. The final step is the manual artery/vein (A/V) labelling.

tubularity values along the paths. Since many of the generated paths are highly overlapping, a filtering step is performed, removing edges, whose paths are entirely enclosed by another path. After this step, a directed over-complete vascular graph, which contains meaningful as well as spurious branches is calculated with sub-voxel accuracy.

2.2 Subtree extraction

Next, anatomically meaningful vessel trees have to be identified. We extract a set of connected subtrees from the over-complete maxima graph G, using an optimization procedure based on an integer program, similar to Türetken et al. [6]. The integer program calculates a configuration of binary variables that minimizes a constrained objective function of weights of adjoining vessel paths. In contrast to their method, we extract multiple trees at a time and do not need explicitly declared root nodes. The root nodes are calculated implicitly by minimizing the objective function, defined as:

$$\begin{aligned} &\arg\min_{t,r} \sum_{e_{ij},\, e_{jk} \in E} w_{ijk}\, t_{ij}\, t_{jk} \;+\; \sigma \sum_{e_{ij} \in E} r_{ij} \\ &\text{s.t.} \quad \begin{array}{ll} \sum_{e_{hi} \in E} t_{hi} + r_{ij} \geq t_{ij}, & \sum_{e_{hi} \in E} t_{hi} + r_{ij} \leq 1, \\ t_{ij} \geq r_{ij}, & t_{ij} + t_{ji} \leq 1, \end{array} \quad \forall e_{ij} \in E \end{aligned} \tag{1}$$

where $t_{ij}, r_{ij} \in \{0,1\}$, $w_{ijk} \in \mathbb{R}$, and $\sigma \in \mathbb{R}_0^+$.

This objective function incorporates two binary variables for each directed edge e_{ij} in the local maxima graph G. The first variable, t_{ij}, is set to 1, if and only if the edge e_{ij} is part of an extracted subtree. The second variable, r_{ij}, is set to 1, if and only if the edge e_{ij} is the root edge of a subtree, i.e., the edge with no predecessors. We use weights w_{ijk} of edge pairs $\langle e_{ij}, e_{jk} \rangle$ instead of weights of single edges to easily incorporate the geometric relation of adjoining edge paths and the weights of single edge paths into one combined weight. This weight needs to distinguish between physically reasonable and unreasonable vessel paths (Figure 2) and is defined as:

$$w_{ijk} = \alpha\, w_{ijk}^{distance} + \beta\, w_{ijk}^{direction} + \gamma w_{ijk}^{radius} + \delta, \tag{2}$$

with $\alpha, \beta, \gamma, w_{ijk}^{distance}, w_{ijk}^{direction}, w_{ijk}^{radius} \in \mathbb{R}_0^+$ and $\delta \in \mathbb{R}^-$.

The first weight of Equation (2), $w_{ijk}^{distance}$, penalizes paths with a large geodesic distance as calculated by the path extraction algorithm. The second weight of Equation (2), $w_{ijk}^{direction}$, takes the geometric relationship of path pairs into account and penalizes path pairs with unusual directions, e.g. paths turning back on themselves. The last weight of Equation (2), w_{ijk}^{radius}, penalizes path pairs, where the radius is increasing. Thus, the correct direction of the path pair is assured. Finally, δ is chosen to be just as negative to make weights of reasonable paths slightly negative, while keeping weights of unreasonable ones positive.

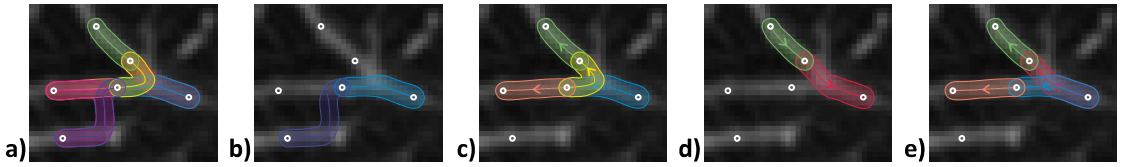

Figure 2: Representative figure showing the function of the edge pair weights in the subtree extraction algorithm. a) All edges detected for a certain region, b) edge pair with high distance weight $w_{ijk}^{distance}$, c) edge pair with high direction weight $w_{ijk}^{direction}$, d) edge pair with high radius weight w_{ijk}^{radius}, e) final edges of a vessel tree.

In our proposed algorithm, the extraction of the subtrees and their root detection is done simultaneously. The edge e_{ij} is the root edge of an extracted subtree, if and only if $r_{ij} = 1$. The second term of Equation (1) limits the number of distinct subtrees by adding a constant value σ for every created subtree increasing the objective function. Therefore, the creation of too many subtrees is prevented while allowing identification of several individual branches.

The combination of the first three constraints of the objective function (1) enforces tree-like structures, by ensuring that each active edge has exactly one predecessor edge, or it is a root edge of a subtree. The fourth constraint in (1) guarantees that if an edge e_{ij} is active, its opposing edge e_{ji} is not active at the same time.

For further processing, the branching points of the actual vessel trees are calculated for each extracted subtree by joining subsequent edges and creating a branching point when two edges, starting at the same vertex, diverge more than 0.1 mm. The paths between two branching points are then linearly resampled with a fixed distance. This leads to the final vessel subtrees, with branching points of the actual vessel and paths of vessel segments with sub-voxel accuracy.

2.3 Manual annotation and analysis of vessel parameters

The extracted vessel trees are manually labelled as either artery or vein by checking their connection to the pulmonary artery or to the left atrium, respectively. Vessel trees consisting of merged arteries and veins or wrongly detected structures are excluded from the analysis. We use the distance metric (DM) as a measure for tortuosity. DM is defined as vessel segment length along the centreline divided by the Euclidean distance between its end points and it is calculated for every vessel segment. These readouts are calculated from contrast-enhanced CT scans of patients who underwent RHC and diagnostic thoracic CT. For this proof-of-concept study we selected patients, who had a clear diagnosis of idiopathic pulmonary arterial hypertension (IPAH, increased pressure in the pulmonary arteries due to unknown reasons), chronic thromboembolic pulmonary hypertension (CTEPH, increased

pressure due to physical obstruction of the pulmonary arteries) or without pulmonary hypertension and presented without comorbidities. The first two groups are marked by an elevated pressure only in the arteries (PH), whereas the last group serves as control (no PH). The DM of the pulmonary arteries, veins and the whole vessel tree is compared for the patient groups with and without PH using Mann-Whitney test. A linear regression analysis with the mean pulmonary artery pressure derived from RHC is performed.

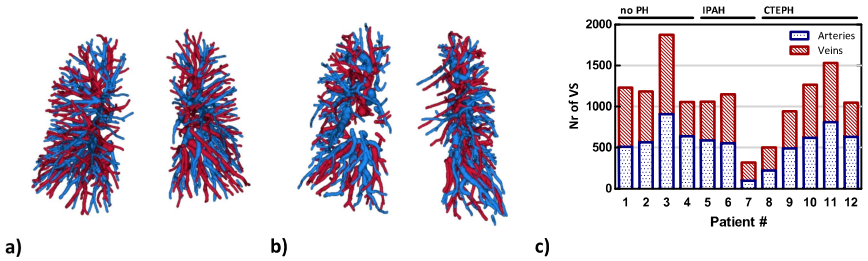

Figure 3: Representative renderings of labelled pulmonary arteries (blue) and veins (red) in a patient a) without and b) with pulmonary hypertension. c) Number of vessel segments (Nr of VS) detected for 4 patients without PH (no PH) and 8 patients with PH (3 IPAH, 5 CTEPH).

3 Results

We selected 12 patients from our dataset with a clear diagnosis (3 patients with IPAH, 5 with CTEPH and 4 without PH). From their thoracic CT images, on average 1100 ± 400 vessel segments were detected (550 ± 220 arterial segments, 540 ± 210 venous segments; Figure 3). On average $3 \pm 2\%$ of voxels were wrongly detected and excluded during the manual annotation. The DM of arteries is significantly higher in patients with PH compared to patients without PH (means: 1.036 ± 0.013 and 1.021 ± 0.001, respectively; Figure 4). In veins the difference is smaller (means: 1.026 ± 0.004 and 1.022 ± 0.001 in patients with and without PH, respectively). Thus in patients with increased pressure on the arterial side, arteries show higher tortuosity than veins. For all vessels combined we find a DM of 1.030 ± 0.007 and 1.022 ± 0.001 for the patients with and without PH, respectively. Further, DM of arteries shows a significant correlation with mPAP, whereas DM of veins does not correlate ($R^2 = 0.50$, $p = 0.011$ vs. $R^2 = 0.32$, $p = 0.06$, respectively; Figure 5). Therefore, the correlation of DM for the combined vessel trees with mPAP ($R^2 = 0.53$, $p = 0.007$) results from the DM of the arteries.

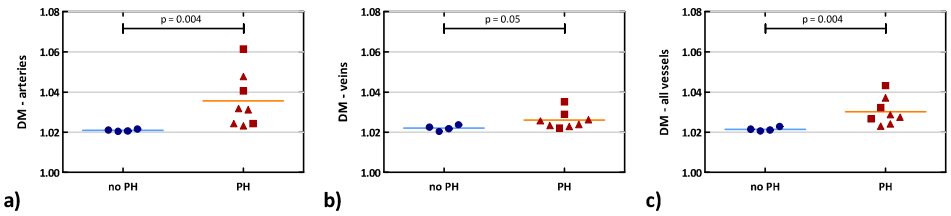

Figure 4: Distance metric (DM) in patients without (no PH: blue circles) and with pulmonary hypertension (PH, IPAH patients: red squares, CTEPH patients: red triangles) for a) the pulmonary arteries, b) veins and c) all vessels combined. Means are shown as lines.

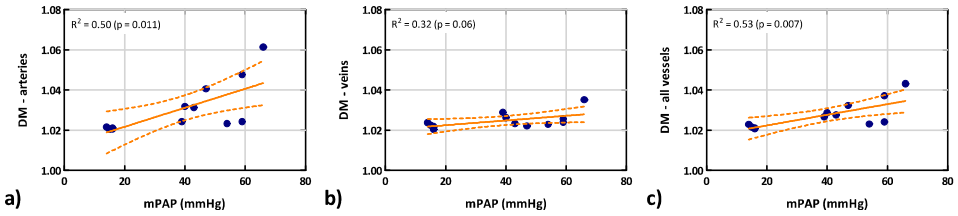

Figure 5: Distance metric (DM) over mean pulmonary artery pressure (mPAP) for a) the pulmonary arteries, b) veins and c) all vessels combined. R = linear correlation coefficient.

4 Conclusion

We present an algorithm that automatically extracts individual pulmonary vessel trees from thoracic CT images. The high confidence of the algorithm is observed by the low number of vessel trees, which had to be excluded in the manual labelling because of merged arteries and veins. Further, the sub-voxel-accuracy of the vessel paths promises an accurate description of the vessel morphology. A limitation of the algorithm is that only vessels with diameters between 2 and 10 mm are considered. Smaller vessels might show further morphological changes, however, are excluded in the present algorithm to limit the runtime.

We find that pulmonary arteries are more bent than veins in patients with increased pressure in the arterial system. Therefore, tortuosity of the arteries and veins may be a useful non-invasive readout for the diagnosis of PH and the distinction between different subtypes of the disease. To facilitate the clinical applicability an automatic artery/vein separation algorithm would be needed, where our vessel extraction algorithm could serve as initial step.

References

[1] Fethallah Benmansour, Engin Türetken, and Pascal Fua. Tubular Geodesics using Oriented Flux : An ITK Implementation. *The Insight Journal*, 2013. doi: http://hdl.handle.net/10380/3398.

[2] Michael Helmberger et al. Quantification of tortuosity and fractal dimension of the lung vessels in pulmonary hypertension patients. *PLoS ONE*, 9(1):e87515, 2014. ISSN 19326203. doi: 10.1371/journal.pone.0087515.

[3] Marius M. Hoeper et al. Definitions and diagnosis of pulmonary hypertension. *Journal of the American College of Cardiology*, 62(25 SUPPL.):D42–D50, 2013. ISSN 07351097. doi: 10.1016/j.jacc.2013.10.032.

[4] Max W. K. Law and Albert C. S. Chung. Three dimensional curvilinear structure detection using optimally oriented flux. In *Lecture Notes in Computer Science (including subseries Lecture Notes in Artificial Intelligence and Lecture Notes in Bioinformatics)*, volume 5305 LNCS, pages 368–382, 2008. ISBN 3540886923. doi: 10.1007/978-3-540-88693-8-27.

[5] David Lesage et al. A review of 3D vessel lumen segmentation techniques: Models, features and extraction schemes. *Medical Image Analysis*, 13(6):819–845, 2009. ISSN 13618415. doi: 10.1016/j.media.2009.07.011.

[6] Engin Türetken et al. Reconstructing loopy curvilinear structures using integer programming. In *Proceedings of the IEEE Computer Society Conference on Computer Vision and Pattern Recognition*, pages 1822–1829, 2013. ISBN 978-0-7695-4989-7. doi: 10.1109/CVPR.2013.238.